Design of a GaN-Based Reconfigurable Resonant Converter for High Frequency On-Board Charger of Battery Electric Vehicles

Manh Tuan Tran[1,2], Haaris Rasool[1,2], Dai Duong Tran[1,2] ,Mohamed El Baghdadi[1,2]
Philippe Lataire[1,2] and Omar Hegazy[1,2*], (Member, IEEE).

[1] Vrije Universiteit Brussel (VUB) & MOBI Research Group, ETEC Department, Pleinlaan 2, 1050 Brussels, Belgium
[2]Flanders Make, 3001 Heverlee, Belgium
*Corresponding author: Omar Hegazy (omar.hegazy@vub.be).

Keywords

«Electric vehicle On-Board charger», «CC-CV (constant current constant voltage) charging», «Reconfigurable resonant network».

Abstract

In this paper, a reconfigurable resonant converter for On-board Chargers (OBCs) and its' design consideration is proposed. This approach allows high frequency operation with maximum efficiency and Zero-Voltage Switching (ZVS) for all primary switches over a wide range of load conditions. The proposed converter is a combination of a Full Bridge LLC (FB-LLC) and an LCL compensator to form a high order resonant network. Constant Current (CC) and Constant Voltage (CV) charging profiles can be implemented automatically by reconfiguring the resonant network on the secondary side. In this design, GaN-FETs and a high frequency planar transformer are employed to further take advantage of high frequency operation. A 300kHz-3.3kW hardware prototype was built. Simulation and experiment results are provided with a maximum efficiency of 97%.

I. Introduction

On-board charger (OBC) is one of the key components in plug-in hybrid electric vehicles (PHEVs) and Battery electric vehicles (BEVs). The automobile industry has recently seen a surge in demand for high power density and efficiency. As a result, increasing switching frequency is required to reduce the size of an OBC system. However, switching losses, conduction losses, and passive component losses, which are proportional to switching frequency, dramatically reduce efficiency. Among several isolated DC-DC topologies for EVs (Electric Vehicles) charging application, LLC resonant emerged as the most promising candidate due to its advantages such as very wide range of zero voltage switching turn-on (ZVS) and Zero current switching (ZCS) turn-off in primary and secondary devices [1][2]. The high efficiency operation maintained around resonant frequency thanks to soft switching achieving and low circulating current. However, in EVs charging applications, a wide range of frequency regulation is required for Constant Current (CC) and Constant Voltage (CV) implementation [2]. This leads to the high ratio of resonant inductor over magnetizing inductor to extend regulation range[3][4]. The efficiency would be degraded due to the high RMS current value and large magnetizing current in resonant tank. In previous work [5], the author introduced a multi-MHz wireless power charger system with a combination of a LCL network [6] and a constant voltage topology, namely S-LCC, to perform a CC-CV charging profile at a fixed resonant frequency. In this study, the proposed approach will be further investigated in On-board charger applications. This paper presents a reconfiguration resonant DC-DC. In which the constant voltage can be easily achieved by a LLC-DCX [7]. For the CC mode, a T-Type LCL is cascaded with an LLC converter on the secondary side of the transformer to convert the constant voltage source into a constant current source. The major characteristics of the proposed converter and contributions of this paper can be summarized as follows:

1) Very simple control strategy for CC-CV implementation without frequency or phase shift modulation. Hence, a larger magnetizing inductance can be designed to reduce the circulating current and make voltage and current gain function less sensitive with a larger tolerance of resonant components.
2) This approach allows more freedom in designing charging specifications for EV applications thanks to its high order resonant network.
3) Optimal magnetic parameters ensure soft-switching ZVS for all primary switches and nearly ZCS for secondary diodes across the entire load range, allowing high frequency and high efficiency operation.
4) Two additional bidirectional switches can be used to minimize conduction losses without any switching losses.
5. A design procedure based on the Multi-Objective Optimazation-based GA (MOGA) framework is developed for proposed coverter.

II. Proposed Reconfigurable Full-Bridge Resonant Converter

The detailed architecture of the proposed on-board charger consists of a front end totem pole Power Factor Correction (PFC) and a back-end reconfigurable resonant converter as illustrated in Fig. 1. The scope of the paper mainly studied the proposed DC-DC converter. To meet the wide range of output voltage requirements as in Fig.3 (a), proposed hybrid resonant topology is a combination of a voltage source converter, which can be LLC or CLLC topology, and a T-type LCL network. The LCL resonant network can be on the primary side or secondary side as depicted in Fig.2 (a), (b), and (c). For high voltage EV battery charger applications, the LCL circuit can be inserted on either the primary or secondary side.

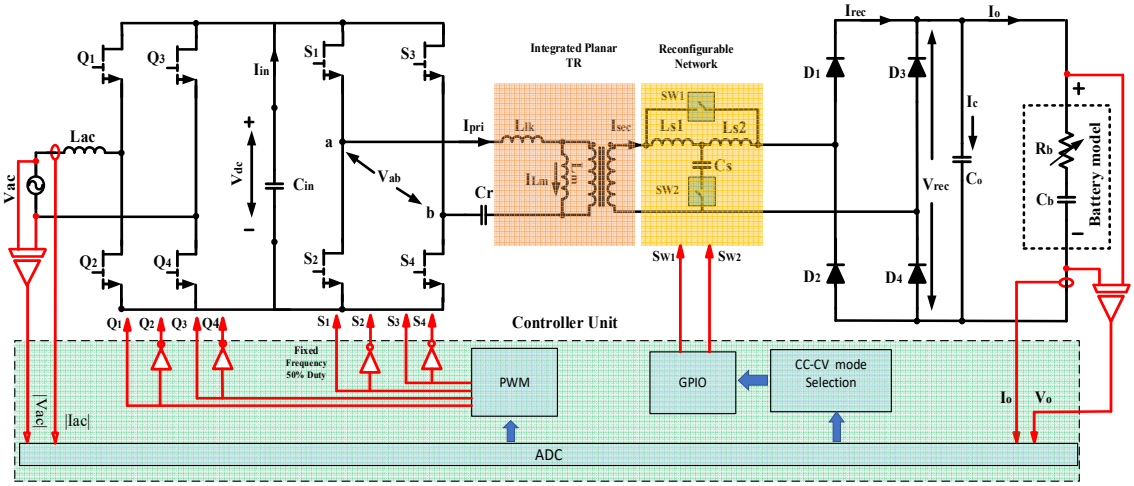

Fig. 1: Configuration of the proposed DC-DC converter system

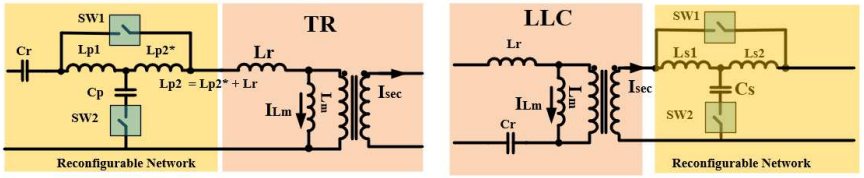

(a) (b)

Fig. 2. Proposed reconfigurable resonant networks for EVs charger system:
(a) configurable network in primary side, (b) configurable network in secondary side.

Compared to the conventional control method for LLC converter, the proposed dc-dc converter with a reconfigurable resonant network allows fulfilling CC-CV operation at a fixed frequency as illustraled in Fig.3 (b). As a result, DC-DC converter stage can operate as a DC transformer (DCX) with a constant gain. Thus, the overall efficiency is maximized. During the CC mode, the bidirectional switch SW_1 is turn OFF and SW_2 is turn ON, the high order resonant network LLC + LCL forms a current source. As battery voltage increase to maximum voltage, SW_1 is turn ON and SW_2 is turn OFF, the converter is configured as voltage source. Thanks to soft-switching operation over the entire load range at the high switching frequency, the GaN (Gallium nitride) Mosfets and Planar Transformer can be used to achieve a high-power density system.

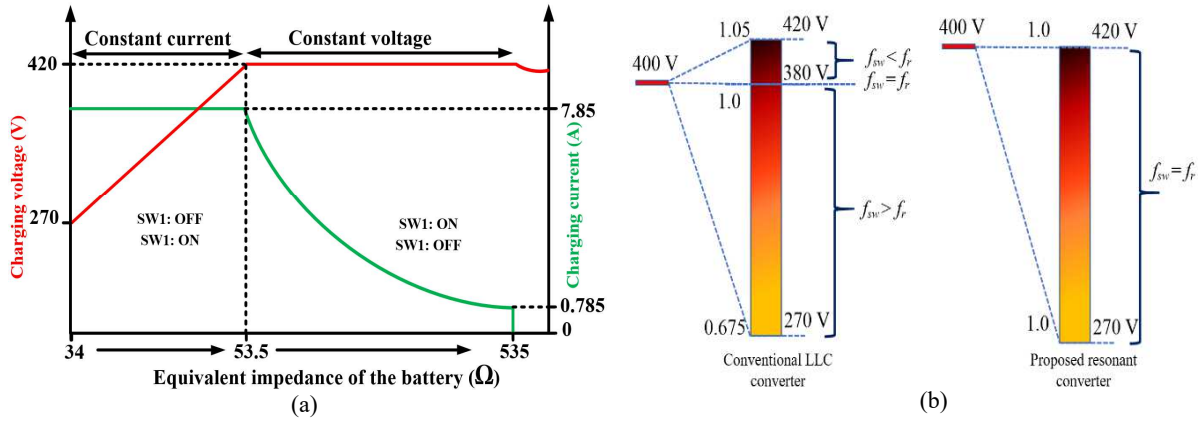

(a) (b)

Fig. 3. (a) Charging specifications , (b) Required voltage range of DC-DC conveter

III. Steady state analysis of proposed DC-DC converter in CC and CV charging mode

The first harmonic approximation (FHA) method is adopted for deriving the steady-state gain function of the proposed converter. The equivalent AC circuits in CC and CV are described as in Fig. 4 and Fig.5. AC input voltage V_{in} is supplied by a full-bridge circuit. Integrated leakage inductor L_r, Magnetizing inductor L_m, C_r, and additional components L_{s1}, L_{s2}, C_2 form a high order resonant network on the primary and secondary sides, respectively. The fundamental components of input voltage V_{in}, output voltage V_{O_ac} and output current I_{O_ac} are derived from (1), (2) and (3). In which, $n = Np/Ns$ is transformer turn ratio.

$$\begin{cases} V_{in} = \dfrac{4V_{dc}}{\pi} \displaystyle\sum_{k=1,3,5}^{\infty} \frac{1}{k}\sin(2\pi k f_{sw} t) & (1) \\ V_{O\_ac} = \dfrac{4nV_O}{\pi} \displaystyle\sum_{k=1,3,5}^{\infty} \frac{1}{k}\sin(2\pi k f_{sw} t - \psi) & (2) \\ I_{O\_ac} = \dfrac{\pi I_O}{2n}\sin(2\pi k f_{sw} t - \psi) & (3) \end{cases}$$

The rms AC equivalent values are calculated as in eq. (4), (5) and (6). The AC equivalent load resistor R_{O_ac} reflected from secondary side can be obtained as in (7).

$$\begin{cases} V_{in_{rms}} = \dfrac{2\sqrt{2}V_{dc}}{\pi} & (4) \\ V_{O_{rms}} = \dfrac{2\sqrt{2}nV_O}{\pi} & (5) \\ I_{O_{rms}} = \dfrac{\pi I_O}{2\sqrt{2}n} & (6) \\ R_{O\_ac} = \dfrac{8n^2 R_O}{\pi^2} & (7) \end{cases}$$

A. Converter configuration for CC charging mode.

As depicted in Fig.4(a), the equivalent AC circuit of CC mode charging is configured by turning ON SW_2, turning OFF SW_1. Where L_r is integrated resonant inductor, L_m is magnetizing inductor of Planar transformer. Additional resonant LCL parameters are reflected into the primary side and denoted as n^2L_{s1}, n^2L_{s2}, C_2/n^2.

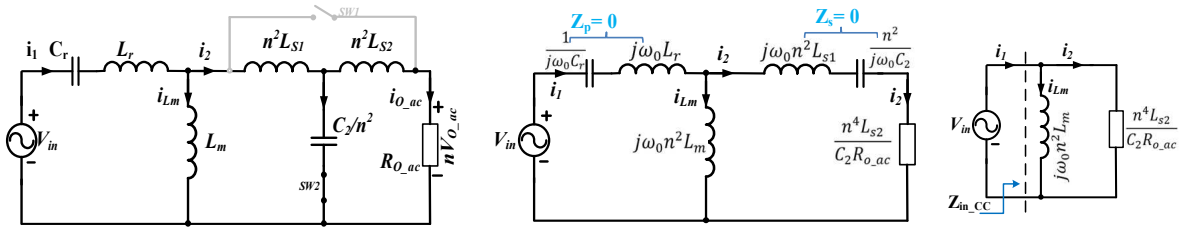

(a) (b) (c)

Fig. 4. Configuration of DC-DC converter in CC mode

$$Z_{eq} = \frac{\dfrac{n^2}{j\omega_0 C_2}(n^2 j\omega_0 L_{s2} + R_{o\_ac})}{\dfrac{n^2}{j\omega_0 C_2} + n^2 j\omega_0 L_{s2} + R_{o\_ac}} = \frac{n^4 L_{s2}}{C_2 R_{o\_ac}} + \frac{n^2}{j\omega_0 C_2} \quad (8)$$

The equivalent impedance Z_{eq} is combined of n^2L_{s2}, C_2/n^2 and R_{o_ac} as calculated in (8). When the conditions are satisfied as in (9), (10). Fig.4 (b) and Fig.4 (c) are deduced to derive output current as in (11). It can be observed from (11) that the output current is independent to the load resistor value. As a result, the constant current is performed at the fixed switching frequency.

$$j\omega_0 L_r + \frac{1}{j\omega_0 C_r} = 0 \quad (9)$$

$$j\omega_0 n^2 L_{s1} + \frac{n^2}{j\omega_0 C_2} = j\omega_0 n^2 L_{s2} + \frac{n^2}{j\omega_0 C_2} = 0 \tag{10}$$

$$\begin{cases} I_2 = \dfrac{V_{in} C_2 R_{o\_ac}}{n^4 j\omega_0 L_{s2}} & (11) \\ I_{O\_ac} = \dfrac{I_2 Z_{eq}}{n^2 L_{s2} + R_{o\_ac}} = \dfrac{V_{in}}{n^2 j\omega_0 L_{s2}} & (12) \\ I_O = \dfrac{8V_{dc}}{\pi^2 n j\omega_0 L_{s2}} & (13) \end{cases}$$

As seen from (13), The DC output current value can be designed based on selecting inductor value L_{s2}. It can be noticed that the higher designed switching frequency will lead to the smaller inductor value.

B. Converter configuration for CV charging mode.

The constant voltage operation can be realized by closing SW_1, and opening SW_2. In this mode, the AC equivalent circuit is configured as conventional LLC topology.

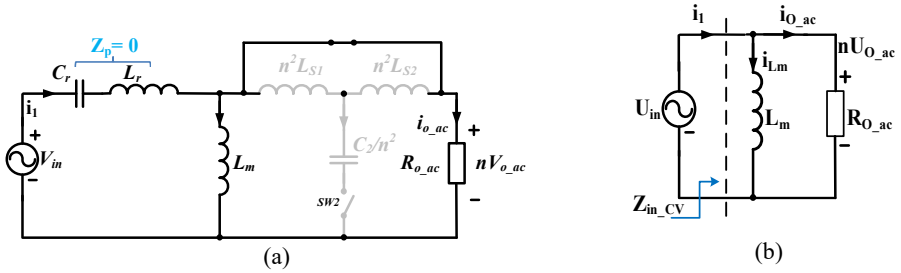

(a) (b)

Fig. 5. Configuration of DC-DC converter in CV mode

Using the fundamental harmonic approximation method for equivalent circuit in Fig.5(a), the input-to-output voltage gain is expressed in (14). And the unity gain can be obtained at resonant frequency ω_0 fulfilled (15).

$$\begin{cases} Gv = \left| \dfrac{\frac{2\sqrt{2}nV_O}{\pi}}{\frac{2\sqrt{2}V_{dc}}{\pi}} \right| = \left| \dfrac{(j\omega_0 L_m)//R_{O\_ac}}{j\omega_0 L_r + (j\omega_0 C_r)^{-1} + (j\omega_0 L_m)//R_{O\_ac}} \right| = \dfrac{nV_o}{V_{in}} = 1 & (14) \\ Z_p = j\omega_0 L_r + \dfrac{1}{j\omega_0 C_r} = 0 & (15) \\ Z_{in\_cv} = \dfrac{j\omega_0 L_m R_{O\_ac}}{j\omega_0 L_m + R_{O\_ac}} & (16) \end{cases}$$

Since the input impedance Z_{in_cv} is a function of load R_{O_ac} and L_m as in (16), the phase of Z_{in_cv} is determined by $arg[Im\{Z_{in\_cv}\}/Re\{Z_{in\_cv}\}] = \arg[-R_{O\_ac}/Z_m]$. Therefore, the most important aspect of the design is to maximize the magnetizing impedance Z_m to minimize the reactive power but still guarantee the soft switching operation. The value of magnetizing inductance is limited as (17) to guarantee the ZVS of primary GAN switches.

$$L_m{}^* \leq \frac{T_d}{8C_{OSS}f_O} \tag{17}$$

The value of L_m is selected by Optimization method as described in the section III.C to ensure the required current fully discharging ouput capacitance C_{OSS} of the switches during deadtime interval T_d.

C. Design procedure and consideration of proposed converter

The designed procedure of the proposed converter is illustrated in Fig.6. The input specifications are defined by the required CC-CV charging profile in Fig.3 (a). Resonant components significantly affect efficiency and power density for the proposed EVs converter design method. Therefore, the Multi-Objectives optimization framework based Matlab environment is built to select the optimal design parameters for resonant components.

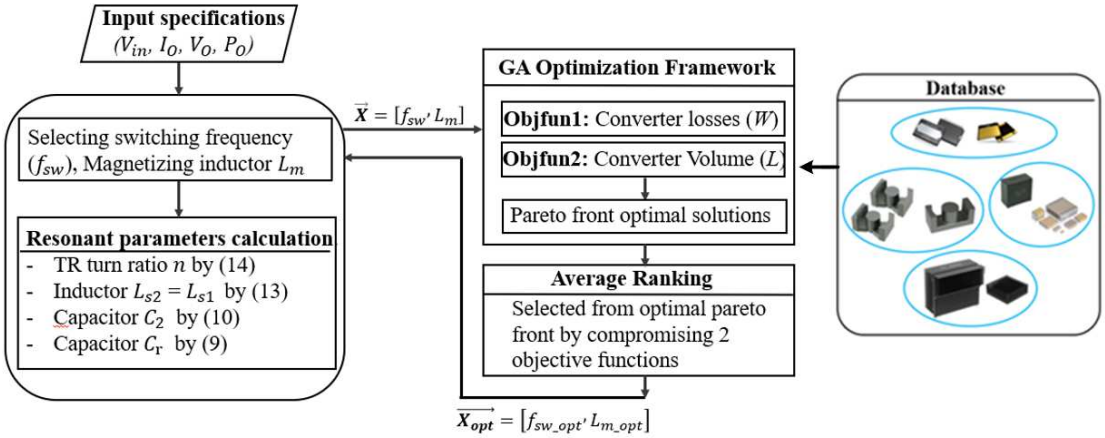

Fig. 6. Design framework of proposed converter system

The design procedure begins by defining input specifications such as input voltage, output voltage, and power rating via created user interface. The optimization algorithm implementation is briefly explained as follows:

Step1. Firstly, the objective functions are defined as (18)

$$Objectives:\ Min \begin{cases} ObjFunc1\ (\vec{X}) = P_{loss}(\vec{X}) \\ ObjFunc2\ (\vec{X}) = Vol(\vec{X}) \end{cases} \qquad Where: \vec{X} = [f_{sw}, L_m] \tag{18}$$

The objective functions of power losses and volume are formulated based on the works in [8][9].

Step2. The constraints and boundary values are selected to generate rational results as given in (19)

$$Subject\ to:\ \begin{cases} 100\ kHz \le fsw\ \le\ 500\ kHz \\ L_m \le\ L_m{}^* \end{cases} \tag{19}$$

Where the boundary value of magnetizing inductance of transformer is defined as in (17)

Step3. Multi Objective Genetic Algorithm (MOGA) is applied to solve the non-convex and multiple objectives. The multi- solutions are presented in a set of Pareto-optimal solutions, as shown in Fig.7

Step4. The average ranking method is utilized to select the most desire solution from the set of Pareto-fronts. A single objective function can be created from two objectives functions by using a weighting factor δ as in (20). For On-board charger system, the power density is critical. In this design, δ coefficient is 0.7, meaning power density has higher priority over power losses. The optimal solution is marked as a red star in Fig. 7.

$$f_{composite} = \delta ObjFunc2\ (\vec{X}) + (1-\delta) ObjFunc1\ (\vec{X}) \qquad Where:\ 0 \le\ \delta\ \le 1 \tag{20}$$

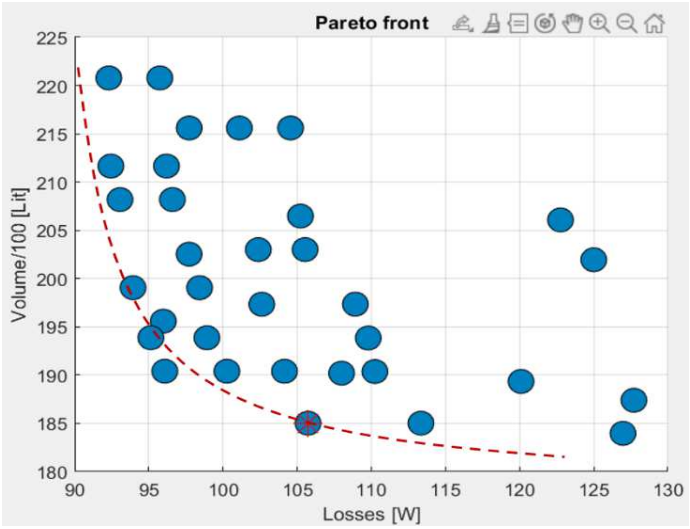

Fig.7 Pareto-front solution

Step5. After launching GA based optimization solver, the optimal parameters of switching frequency f_{sw_opt} and L_{m_opt} is obtained. According to the (13), (12), (10) and (9), the resonant parameters are calculated as (21)

$$\begin{cases} L_{s1} = L_{s2} = \dfrac{8V_{dc}}{\pi^2 n j \omega_{opt} I_O} \\ C_2 = \dfrac{1}{(\omega_{opt})^2 L_{s2}} \\ C_r = \dfrac{1}{(\omega_{opt})^2 L_r} \end{cases} \tag{21}$$

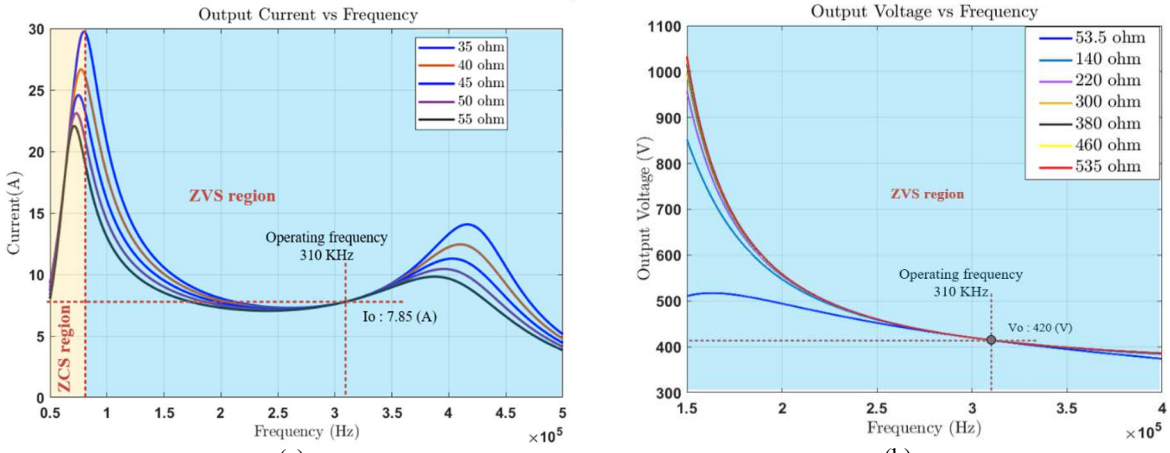

(a) (b)

Fig. 8. Gain curve according to load resistor and frequency: (a) Current gain, (b) voltage gain

To validate selected parameters, the output voltage and the output current curves versus the operating switching frequency with various loads are plotted in Fig. 8. The charging values of the converter are maintained constant at resonant frequency regardless of load conditions. Hence, the proposed design method is suitable to implement CC-CV charging for battery charring applications.

IV. Simulattion and Experiment Results

In this section, simulation model is built by PSIM to validate the key waveforms of proposed converter as illustrated in Fig.9. The experiment results are then povided by a 300kHz- 3.3kW reconfigurable resonant converter prototype as shown in Fig.10. Design parameters of resonant components are listed in Table I. There is a small deviation between simulated and practical parameters. Therefore, the output value is correctified by slightly adjusting the switching frequency to guarantee operating at a resonant point.

Table I: Specification and components of proposed converter

Parameters	Symbols	Values
Power	P_O	3.3 kW
Input voltge	V_{in}	400 V
Output Voltage	V_{out}	270V-420V
Transformer's turn ratio	N_P/N_S	*1.12*
Switching frequency	f_{sw}	*300 kHz*
Primary inductor	L_r	*2.8 uH*
Magnetizing Inductor	L_m	*50uH*
Additional secondary inductors	L_{s1}, L_{s2}	22 *uH*
Primary capacitor	C_r	94 *nF*
Additional Secondary capacitor	C_2	14.2 *nF*
Components	Symbols	Part number
Pimary GAN switches	$S_1 - S_4$	GS66508T
Secondary rectifier Schottky diodes	$D_1 - D_4$	SCS230AE2

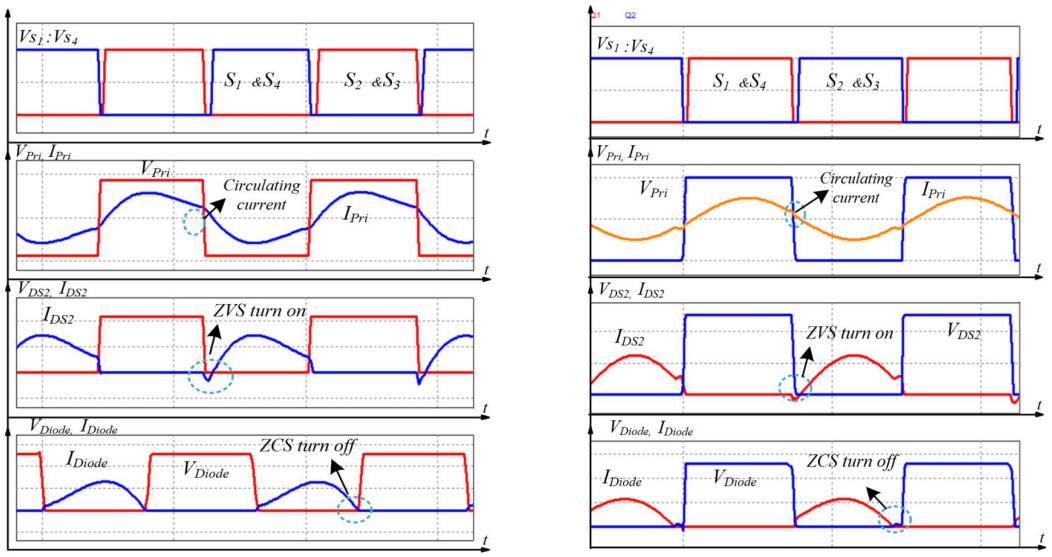

(a) (b)

Fig. 9. Key waveforms of the proposed converter in CC mode (a), and CV mode (b)

The soft switching characteristics of the proposed converter are satisified in both CC mode and CV mode as shown in Fig.9. Where ZVS for all primary devices and ZCS for secondary diodes are clearly demonstrated.

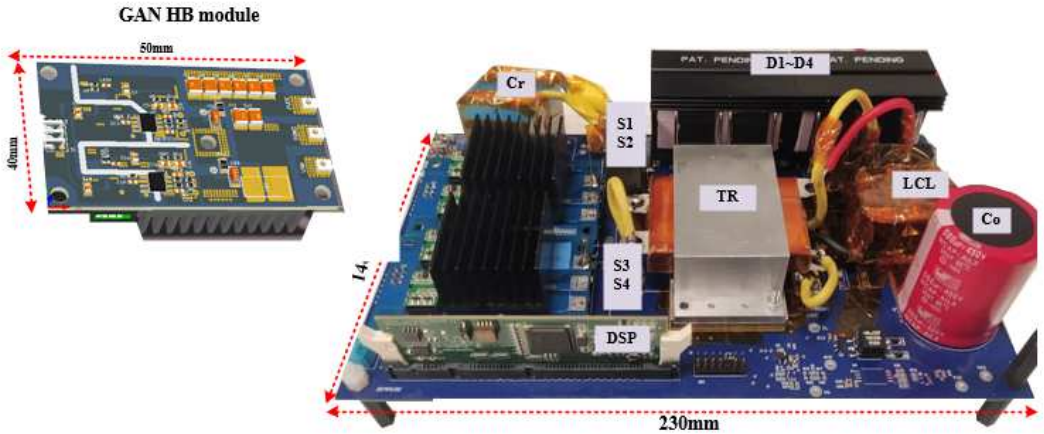

Fig. 10. Photograph of the prototype DC-DC converter

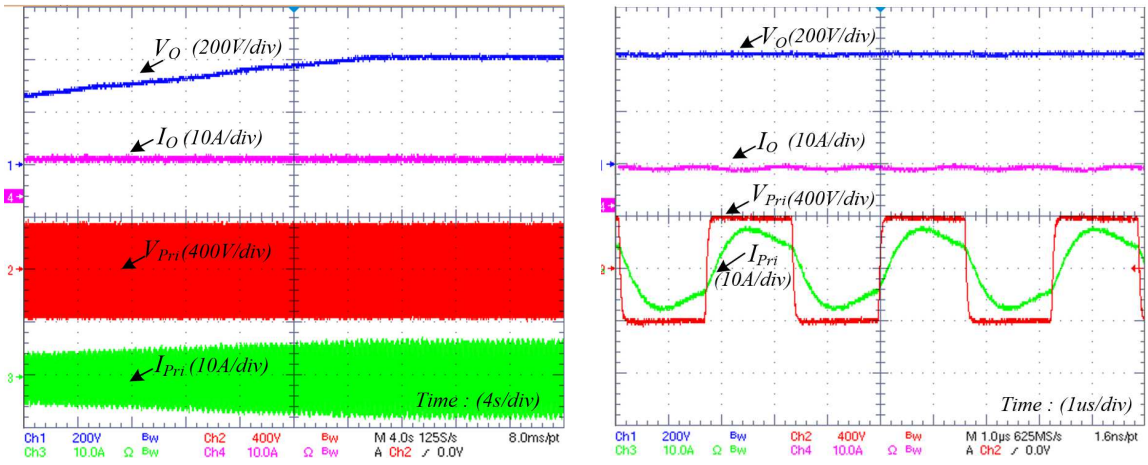

(a) (b)

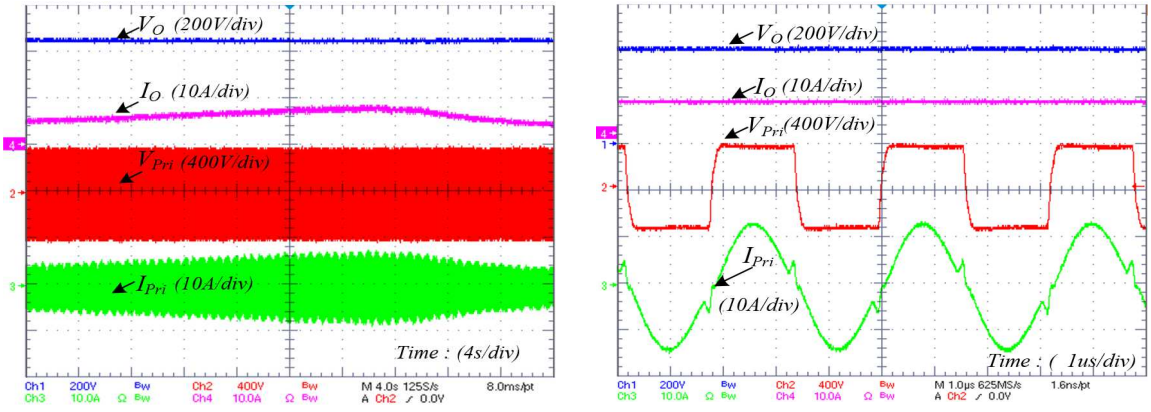

(c) (d)

Fig.11. Experiment results 3 kW with variable resistor load: (a) Constant current performance, (b) Key waveforms in CC mode, (c) Constant voltage performance, (d) Key waveforms in CV mode

As shown in Fig.11, the constant current and constant voltage charging can be performed at a fixed frequency of 310 kHz. The output current of 7.8 A is kept constant during CC mode regardless of load variation as in Fig. 11(a). Fig.11 (b) shows that the primary current leads primary voltage, and the ZVS condition is achieved. While Fig.11 (c) shows the constant voltage of 420 V with key waveforms zoomed in Fig.11 (d).

V. Conclusion

In this paper, a GaN-Based reconfigurable DC-DC converter has been proposed for On-board charger applications. The CC/CV charging profile is performed without a dedicated controller design. The converter operates at the fixed-high switching frequency and optimal condition to maximum efficiency thank to proposed reconfigurable network. The optimization design framework is developed for sizing passive components, which contributed a substantial portion of the overall volume of the converter. The design methodology of the 3.3kW DC-DC converter is validated at switching frequency of 300 kHz hardware prototype with a peak efficiency 97.5%.

ACKNOWLEDGEMENT

This research has received funding from the European Union's Horizon 2020 research and innovation programme under grant agreement No 101006943, under the title of URBANIZED (https://urbanized.eu/). We also acknowledge Flanders Make for the support to our research group.

.

References

[1] D. Junjun, L. Siqi, H. Sideng, C. C. Mi, and M. Ruiqing, "Design methodology of LLC resonant converters for electric vehicle battery chargers," IEEE Trans. Veh. Technol., vol. 63, no. 4, pp. 1581–1592, May 2014.

[2] F. Musavi, M. Craciun, D. S. Gautam and W. Eberle, "Control Strategies for Wide Output Voltage Range LLC Resonant DC–DC Converters in Battery Chargers," in *IEEE Transactions on Vehicular Technology*, vol. 63, no. 3, pp. 1117-1125, March 2014, doi: 10.1109/TVT.2013.2283158.

[3] R. Beiranvand, B. Rashidian, M. R. Zolghadri and S. M. Hossein Alavi, "A Design Procedure for Optimizing the LLC Resonant Converter as a Wide Output Range Voltage Source," in *IEEE Transactions on Power Electronics*, vol. 27, no. 8, pp. 3749-3763, Aug. 2012, doi: 10.1109/TPEL.2012.2187801.

[4] R. Beiranvand, B. Rashidian, M. R. Zolghadri and S. M. H. Alavi, "Using LLC Resonant Converter for Designing Wide-Range Voltage Source," in *IEEE Transactions on Industrial Electronics*, vol. 58, no. 5, pp. 1746-1756, May 2011, doi: 10.1109/TIE.2010.2052537.

[5] M. T. Tran and W. Choi, "Design and Implementation of a Constant Current and Constant Voltage Wireless Charger Operating at 6.78 MHz," in *IEEE Access*, vol. 7, pp. 184254-184265, 2019, doi: 10.1109/ACCESS.2019.2959981.

[6] M. Borage, K. V. Nagesh, M. S. Bhatia and S. Tiwari, "Resonant Immittance Converter Topologies," in *IEEE Transactions on Industrial Electronics*, vol. 58, no. 3, pp. 971-978, March 2011, doi: 10.1109/TIE.2010.2047835.

[7] T. M. Tuan and W. Choi, "A Novel Two-Stage Power Conversion Method suitable for LDCs of the Electric Vehicles," *2019 10th International Conference on Power Electronics and ECCE Asia (ICPE 2019 - ECCE Asia)*, 2019, pp. 1-7, doi: 10.23919/ICPE2019-ECCEAsia42246.2019.8797020.

[8] Z. Li *et al.*, "A High-efficiency DC/DC Converter with SiC Devices and LLC topology for Charging Electric Vehicles," *2018 Asian Conference on Energy, Power and Transportation Electrification (ACEPT)*, 2018, pp. 1-7, doi: 10.1109/ACEPT.2018.8610743.

[9] H. -N. Vu, M. Abdel-Monem, M. El Baghdadi, J. Van Mierlo and O. Hegazy, "Multi-Objective Optimization of On-Board Chargers Based on State-of-the-Art 650V GaN Power Transistors for the Application of Electric Vehicles," *2019 IEEE Vehicle Power and Propulsion Conference (VPPC)*, 2019, pp. 1-6, doi: 10.1109/VPPC46532.2019.8952196.